Contract No:

This document was prepared in conjunction with work accomplished under Contract No. DE-AC09-08SR22470 with the U.S. Department of Energy (DOE) Office of Environmental Management (EM).

Disclaimer:

This work was prepared under an agreement with and funded by the U.S. Government. Neither the U. S. Government or its employees, nor any of its contractors, subcontractors or their employees, makes any express or implied:

1) warranty or assumes any legal liability for the accuracy, completeness, or for the use or results of such use of any information, product, or process disclosed; or
2) representation that such use or results of such use would not infringe privately owned rights; or
3) endorsement or recommendation of any specifically identified commercial product, process, or service.

Any views and opinions of authors expressed in this work do not necessarily state or reflect those of the United States Government, or its contractors, or subcontractors.

We put science to work.™

Savannah River
National Laboratory ™

OPERATED BY SAVANNAH RIVER NUCLEAR SOLUTIONS

A U.S. DEPARTMENT OF ENERGY NATIONAL LABORATORY • SAVANNAH RIVER SITE • AIKEN, SC

Characterization of Oxyhydroxides on a Dry-Stored Fuel Plate From L-Basin

L. Olson, R. Fuentes, A. d'Entremont, R. Sindelar

October 2018

SRNL-STI-2018-00428, Revision 0

SRNL.DOE.GOV

DISCLAIMER

Printed in the United States of America

Prepared for
U.S. Department of Energy

Characterization of Oxyhydroxides on a Dry-Stored Fuel Plate From L-Basin

L. Olson
R. Fuentes
A. d'Entremont
R. Sindelar

October 2018

Savannah River
National Laboratory ™

OPERATED BY SAVANNAH RIVER NUCLEAR SOLUTIONS

REVIEWS AND APPROVALS

AUTHORS:

_____
Luke C. Olson, Materials Applications and Process Technology, SRNL   Date

_____
Roderick E. Fuentes, Corrosion and Materials Performance, SRNL   Date

_____
Anna L. d'Entremont, Energy Materials, SRNL   Date

_____
Robert L. Sindelar, Materials Science and Technology, SRNL   Date

TECHNICAL REVIEW:

_____
Poh-Sang Lam, Corrosion and Materials Performance, SRNL   Date

APPROVAL:

_____
Marissa M. Reigel, Manager   Date
Materials Applications and Process Technology, SRNL

_____
Kristine E. Zeigler, Manager   Date
Materials Science and Technology, SRNL

_____
Michael J. Connolly, Idaho National Laboratory   Date

TABLE OF CONTENTS

LIST OF FIGURES

LIST OF ABBREVIATIONS

ASNF	Aluminum-Clad Spent Nuclear Fuel
BSD	Backscatter Electron Detection
EDS	Energy Dispersive Spectroscopy
FESEM	Field Emission Scanning Electron Microscopy
LEU	Low-Enriched Uranium
MTR	Material Test Reactor
SEM	Scanning Electron Microscopy
SRNL	Savannah River National Laboratory
SRS	Savannah River Site
XRD	X-Ray Diffraction

1.0 Executive Summary

This report describes the characterization of oxyhydroxide (oxide) films on a fuel plate that was previously irradiated in an RU-1 pool type reactor in Uruguay and subsequently stored in vented dry storage, first in Uruguay and most recently in L-Area on the Savannah River Site. Characterization of the as-received oxides includes the oxide morphology, thickness, structure, and chemical composition. The results from this work will, in a future report, be compared to characterizations of oxide films grown on alloys in the laboratory under prototypic conditions. The aim is to validate laboratory-grown oxyhydroxides as representative surrogates for further studies for response under drying and radiation conditions.

The work in this report is interim results and preliminary information prepared under Task 6, Milestone 6.2 in Task Technical and Quality Assurance Plan SRNL-RP-2018-00610. Additional experimental milestones are in progress and will be reported upon completion.

- XRD analysis revealed gibbsite as the predominant oxide on the fuel plate surface. It is possible that some boehmite may be present, as well, however the peak appears shifted.
- Most of the surface characterized appeared to have only very thin oxide (on the order of 200 nm thick). There was difficulty observing the thin oxide cross-sections on an as-cut sample, possibly due to damage or contamination from the mounting process, but they were observable in a nickel-plated sample.
- Areas with thicker oxides up to 22.3 µm thick were observed sparsely on the surface but appear to be outliers.
- The oxide morphology appears to be blocky and dense in both thin and thick oxide regions, which is expected to be more protective than a porous film.

2.0 Introduction

2.1 Motivation for Sampling Oxyhydroxides on L-Basin Fuel

Oxide films can be grown consistently under controlled laboratory environments; however, the value of data generated from tests on laboratory-grown oxides requires that specimens match the oxides observed on actual Aluminum-Clad Spent Nuclear Fuel (ASNF) cladding in both structure and composition. Therefore, the motivation for oxyhydroxide sampling on actual ASNF is to identify and characterize (quantify) oxyhydroxides present on ASNF cladding and thereby provide a benchmark for analyses performed on laboratory-grown oxides on aluminum substrates. Analysis of oxide structure, morphology, and composition will be used to establish whether laboratory-grown surrogate materials are representative of the in-service oxides.

2.2 RU-1 Reactor Fuel Plate Exposure and Storage History

Validation activities using FY17 funding support the characterization and testing of oxides sampled from a Material Test Reactor (MTR) fuel plate from the 10-kW RU-1 pool type reactor in Uruguay. Fuel plates from the RU-1 reactor contain low-enriched uranium (LEU) and are clad in Al-1100. The fuel plate was in the reactor core for approximately 8 years total, 5.75 years under power.[1] Upon discharge from the reactor and prior to shipment to Savannah River Site (SRS), the RU-1 fuel was stored dry and in ambient air in Uruguay for about 11 years. After transport to SRS, the fuel was continuously stored dry and in ambient air for 20 years, first in K-Area and later in L-Area. The condition of this fuel has been documented through video and still photographs as part of a fuel inspection program (Figure 1). Due to the low power of the RU-1 research reactor, and an estimated cladding temperature of around 70°C during operation, this fuel is

expected to have a thin oxide layer that is composed primarily of aluminum trihydroxide (gibbsite and/or bayerite).
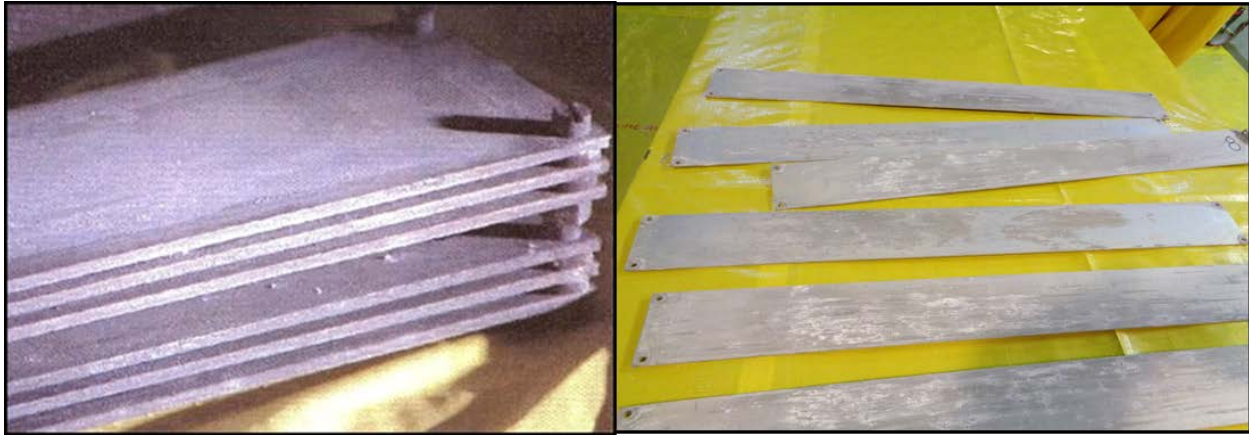

Figure 1 Plate fuel bundle (left) and debundled plates (right) from Uruguay RU-1 Pool Reactor.

2.3 <u>Literature Models</u>

To orient expectations for the oxide thickness and morphology of the RU-1 plate, a literature search was performed. Some important parameters that could inform modeling from the Uruguay reactors are unknown, such as pool pH, chemistry control, and cooling flow rate past the fuel. However, comparable test data and literature models were found, given the following assumptions: low to no flow at ~70 °C, 5 to 8 pH, oxygen-saturated water, 5.75 years of exposure time (ignoring unpowered operation time).

Draley et al. measured the corrosion of 1100 aluminum in oxygen-saturated waster at 70 °C at a 6.5 pH for up to 1.5 years, using two corrosion vessels.[2] Each vessel tested contained multiple samples. The water in the first vessel was refreshed with fresh water while the second received water from the first vessel (carrying corrosion products from the corrosion in the first vessel). It was found that the long-duration behavior was logarithmic, and the data was fitted in the form

$$L = a \log_{10}\left(\frac{t}{1 \text{ day}}\right) + b$$

where L is mass of metal corroded per unit surface area in mg/dm^2, t is the exposure time in days, and a and b are fitted constants.

The expression to convert from the metal loss per area L to oxide thickness x_{ox}, assuming a dense and completely adherent film, is given by

$$x_{ox} = \frac{L}{M_{Al}} \frac{M_{ox}}{\rho_{ox}}$$

where $M_{Al} = 27$ g/mol and M_{ox} are the molar masses of Al metal and oxide and ρ_{ox} is the oxide density. For gibbsite (as found on the RU-1 sample), $M_{ox} = 78$ g/mol and $\rho_{ox} = 2.42$ g/cm^3.[3]

The average fits reported and the corresponding predictions for metal loss and dense film thickness after 5.75 years (2099 days) are in Table 1. The reported fits were significantly different between the two vessels,

but similar among specimens in the same vessel. The actual oxide film might be porous, which would tend to increase the thickness for a given mass of oxide.

Table 1 Literature model parameter values from reference [2] and calculated oxide thickness for the RU-1 plate.

Vessel	a (mg/dm^2)	b (mg/dm^2)	L(2099 days) (mg/dm^2)	x_{ox}(2099 days) (dense film) (μm)
1	3.23	35.59	46.3	5.53
2	2.78	30.20	39.4	4.70

Additionally, in Draley et al. [2], the authors refer to some of their previous findings of aqueous corrosion of 1100, stating that "After sufficiently extended exposure, bits of the corrosion product slough or flake off, leaving a metallic sheen. The corrosion product does not again grow thick in those places, and there is no observable increase in corrosion of the specimens."

Shorter duration tests were later performed by the same authors, but for 45 days at 70 °C, in oxygen-saturated and helium-saturated water.[4] The results are tabulated in Table 2.

Table 2 Literature model parameter values from reference [4] and calculated oxide thickness for the RU-1 plate.

	a (mg/dm^2)	b (mg/dm^2)	L(2099 days) (mg/dm^2)	x_{ox}(2099 days) (dense film) (μm)
O_2-sat.	3.65	36.76	48.9	5.84
He-sat.	3.42	37.83	49.2	5.87

Kim et al. reported in-reactor exposure at ~70 ± 20 °C, with heat flux and coolant flow velocity of 8-9 m/s, yielded oxides about 10-40 µm thick after ~150-300 days.[5] In another paper, Kim et al. gives a single data point for oxide thickness of 43±7 µm resulting from in-reactor exposure for ~500 days at a temperature varying from about 75°C down to around 50°C, with 6.5 pH, variable heat flux, and water flow velocity of 6.6 m/s.[6]

3.0 Oxyhydroxide Characterization and Analysis

3.1 <u>Sample Preparation</u>

A single, dry-stored RU-1 fuel plate was shipped to SRNL for analysis and testing (Figure 2). Four cladding samples were cut from the end of plate using mechanical shears such that internal LEU fuel meat was not exposed (Figure 3). One sample was retained as a spare in storage; one was analyzed with X-ray diffraction (XRD) and then later used for plan-view imaging using contained scanning electron microscopy (SEM), and the other two samples were mounted and prepared for cross-sectional imaging using field emission SEM (FESEM) (Figure 4). Of the two samples prepared for FESEM, one had its oxide surface nickel-plated prior to mounting while the other was mounted without the addition of nickel-plating.
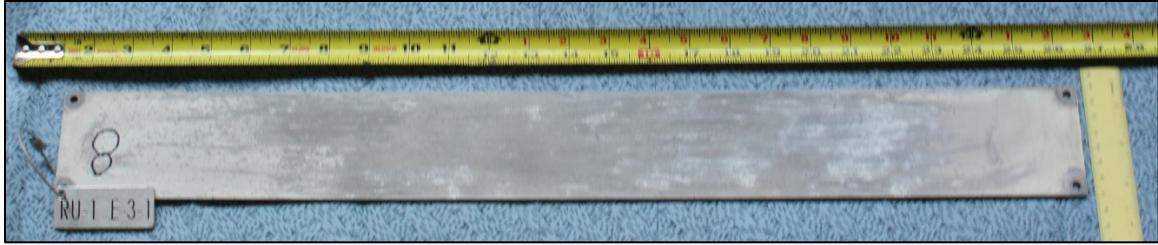
Figure 2 As-received Uruguay RU-1 fuel plate prior to characterization at SRNL.
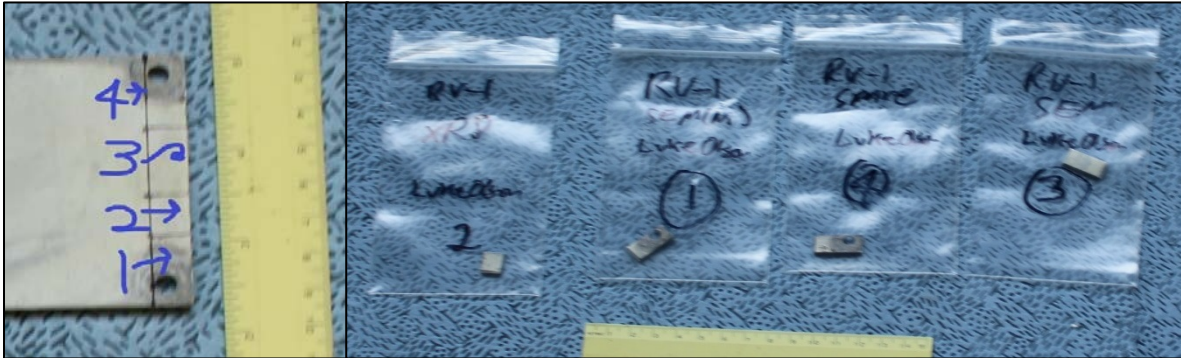
Figure 3 (Left) Location of samples on fuel plate; (right) samples used in characterization: XRD and plan-view SEM, nickel-plating + FESEM, spare, FESEM.

Shearing the fuel plate with mechanical shears did result in some distortion of the fuel plate (Figure 4). Visually, it appears that oxides survived the shearing process (Figure 5).
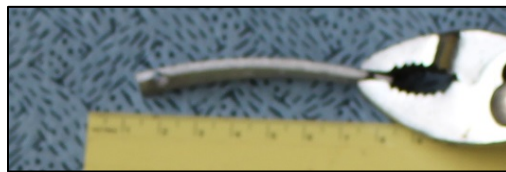
Figure 4 Distortion from shearing.

Figure 5 Oxides on sample to be nickel-plated.

The as-cut and nickel-plated coupons for FESEM were mounted together in EpoFix. Glass slides were placed between samples in the epoxy mount to reduce pressure on the samples during grinding and polishing.

Nickel plating was applied to the surface of sample 1 (Figure 3) using a Caswell Electroless nickel-plating system with application conditions of 1 hour at a temperature of 95 °C.[7] Caution is warranted in analysis of the nickel-plated sample data because the nickel-plating process may affect the native oxide coating. The elevated temperature may have altered the oxide chemistry and morphology. The electroless nickel-plating process results in a nickel plating with ~5 to 10% phosphorus. Most of the surface appeared to be

successfully plated; however, some regions did not appear to plate as well. It is believed that these regions where nickel-plating was difficult correspond to regions of thicker oxide. The thicker oxide on the nickel-plated coupon may be partially due to localized corrosion from the bolt/screw used to hold the fuel bundle together post discharge and, as a result, may not be representative of oxide on the normal plate surface.

3.2 <u>XRD Analysis</u>

X-ray diffraction was performed on sample 2 as identified in Figure 3. The resulting spectra are shown in Figure 6 and Figure 7.
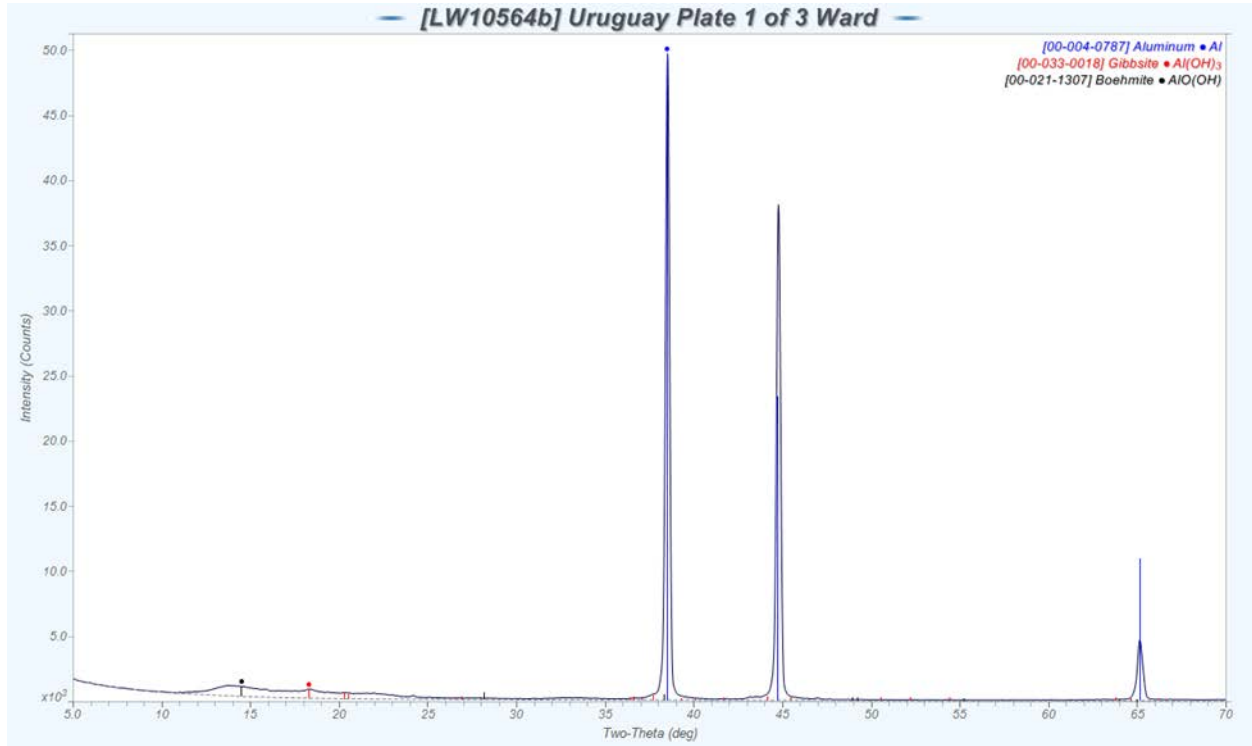

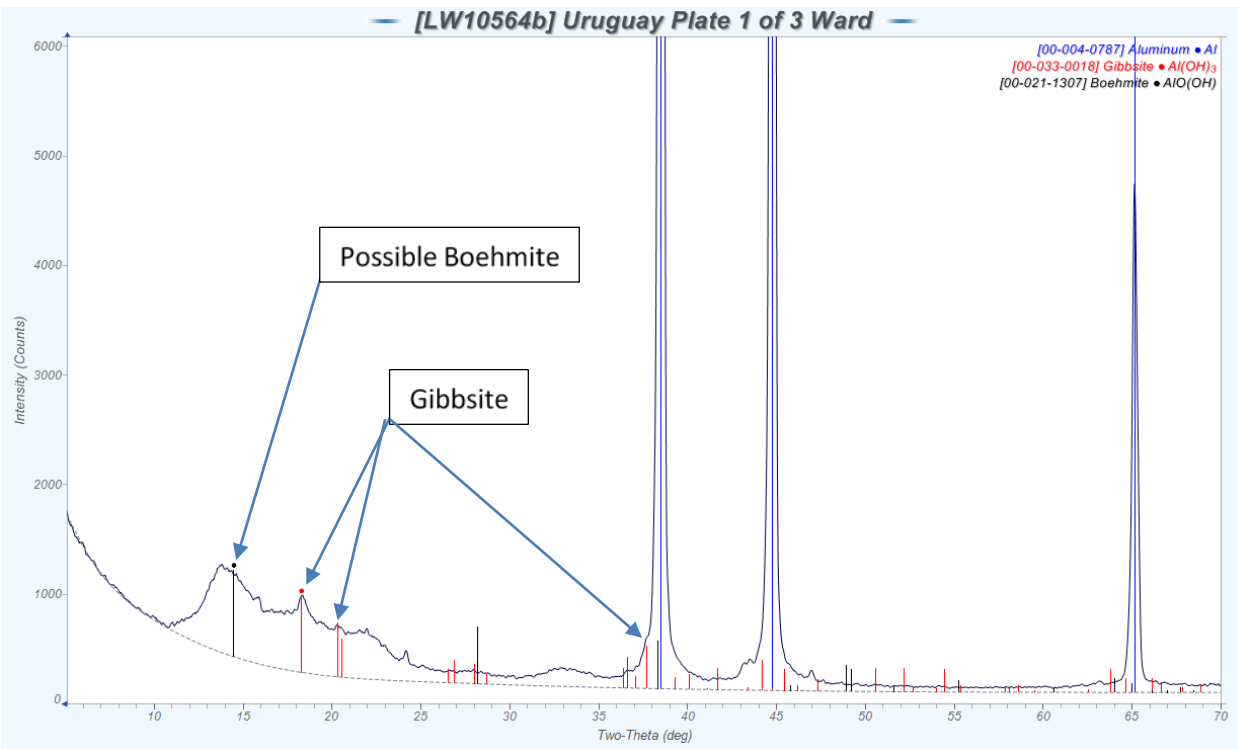**Figure 6 XRD spectrum of Sample 3 oxide.**

Figure 7 Scale adjusted XRD spectrum of Sample 3 oxide to more clearly show the oxide peaks.

The XRD analysis detected the base aluminum metal as well as a layer of gibbsite on the surface. This is expected since the RU-1 pool type reactor operated at low power, 10 kW, and the surface of the cladding was expected to be ~70 °C in service. Trihydroxides such as gibbsite form at temperatures below ~80 °C [8]. A shifted peak at 15 degrees may correspond to boehmite on the sample; however, this identification was less certain and would be unexpected given the known service and extended storage history.

Characterization of surrogate oxides grown on Al 1100 using a hot-wall immersion method at 50 °C [9] identified the oxide as bayerite, another trihydroxide polymorph. Oxides grown on Al-6061 under similar conditions [10] were also identified as predominantly bayerite, possibly accompanied by a smaller amount of gibbsite. The specific trihydroxide polymorphs formed for corrosion below ~80 °C have been found to depend on environmental characteristics such as pH and/or presence of impurities in the water, with bayerite formation associated with the absence of impurities and near-neutral pH (~5.8 to ~9) while gibbsite was associated with the presence of impurities (such as solutions of NaOH or KOH) or high (>9) or low (<5.8) pH [3, 8].

3.3 FESEM on as-sheared (unplated) sample

Sample 3 (Figure 3) was mounted in EpoFix without the application of a nickel plating to the oxide surface. A gap was observed to be present between the sample and the mounting material along the entire edge of the sample, Figure 8 and Figure 9. It is believed that the EpoFix mount medium likely pulled away from the oxide surface during curing to produce this gap.
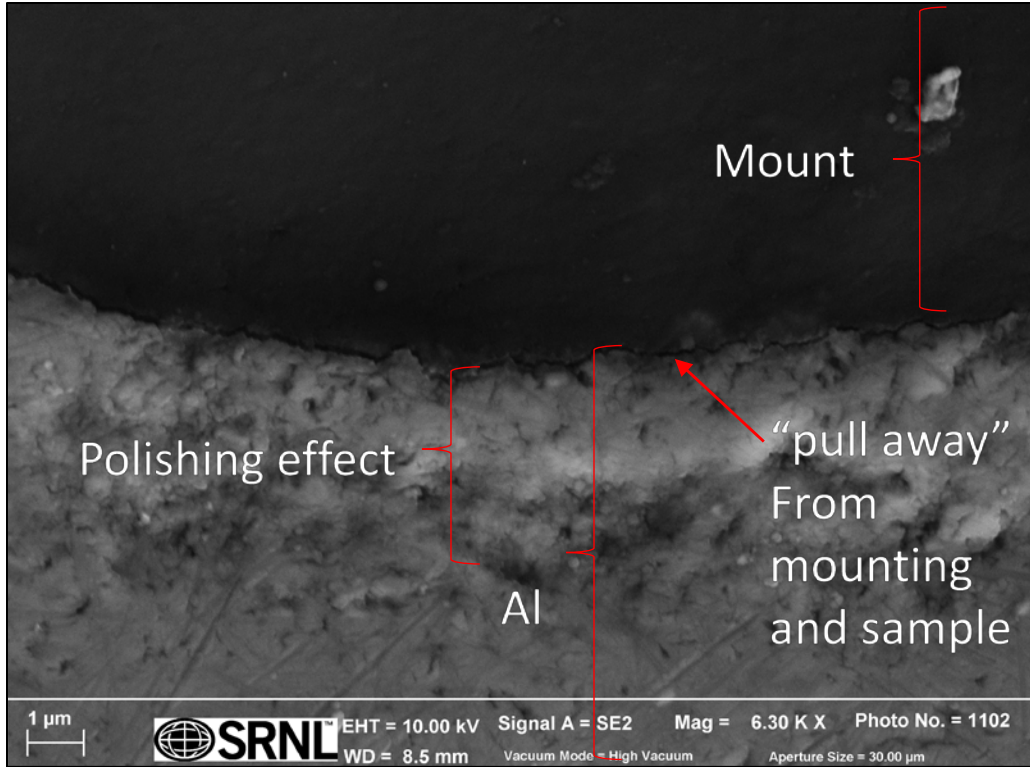
Figure 8 Sample 3 SEM image for topological information (6.3kX magnification).
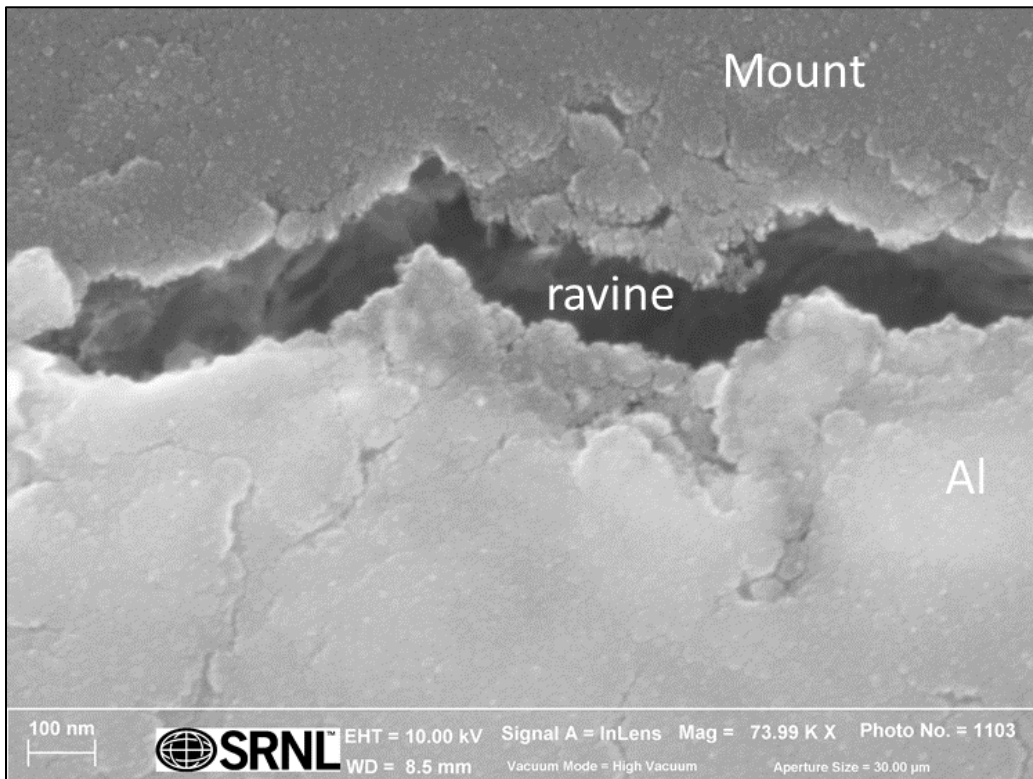

Figure 9 Sample 3 In-lens image reveals "pull away" between mount & sample (74kX magnification).

In other cross-sectioned SEM images of Sample 3, there is ambiguity between oxide and polishing debris. Debris could be introduced if the mount medium were to infiltrate the oxide or if polishing-related liquids infiltrated cracks in the oxide surface. The EDS results of these regions did reveal some oxide content (Figure 10). The EDS results should be interpreted with caution. In general, EDS spatial resolution can often be assumed to range from a micron to several microns in diameter on sample surface and into the sample.[11] More accurately, the spatial resolution is a function of the sample chemistry, density, and SEM accelerating beam voltage.[12] Using the Anderson and Hasler model for x-ray generation range, the spatial resolution for Al and O in a material with a density of 2.7 g/cm^3 (aluminum) is about 3.6 µm, but the spatial resolution for Al and O in a material with a density of 4 g/cm^3 (Al_2O_3) is about 2.5 µm.[12] In Figure 10, the O/Al ratios at EDS points 3 (O/Al=2.8), 4 (O/Al=2.9), and 5 (O/Al=1.9) are consistent with $Al(OH)_3$ (gibbsite or bayerite), $Al(OH)_3$ (gibbsite or bayerite), and AlOOH (boehmite), respectively.

All results in atomic%			
Spectrum O	Al	S	Cl
1 4.6	95.4		
2 90.4		4.1	5.4
3 73.7	26.3		
4 74.4	25.6		
5 63.6	33.9	2.5	

blue: aluminum
Yellow: mount
orange: aluminum oxide
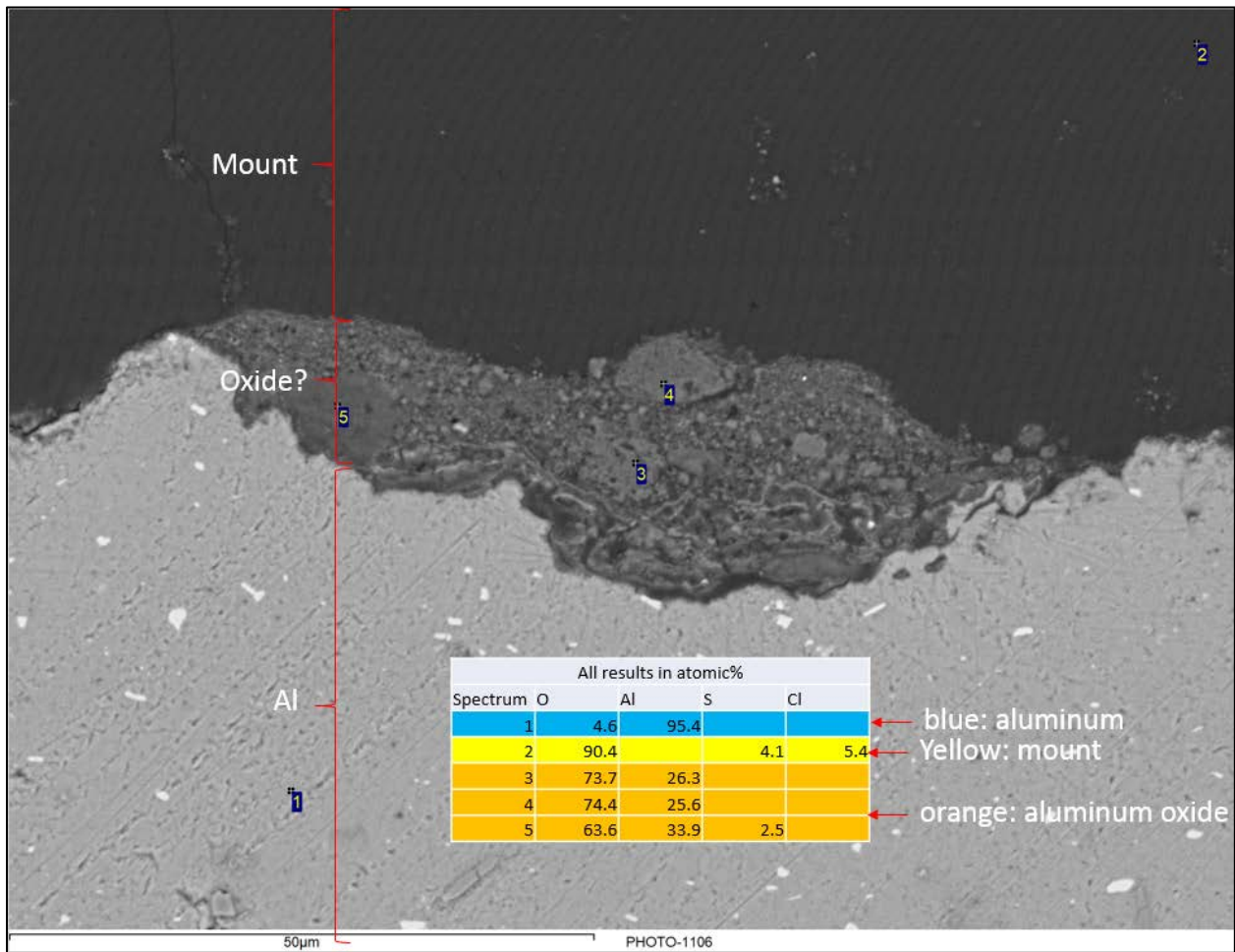
Figure 10 Backscatter Electron Detection (BSD) image showing possible oxide layer at 1080X magnification.

Another potential oxide is shown in Figure 11. In Figure 11, the O/Al ratio of the oxide at EDS point 2 is 2.9, which is consistent with a trihydroxide, $Al(OH)_3$ (gibbsite or bayerite). Image postprocessing, using the software package ImageJ, was used to determine the cross-sectional thickness of the oxide. In Figure 10, the oxide thickness ranged from 5.6 µm to 22.3 µm; in Figure 11, the oxide thickness ranged from 3.1 µm to 7.3 µm.
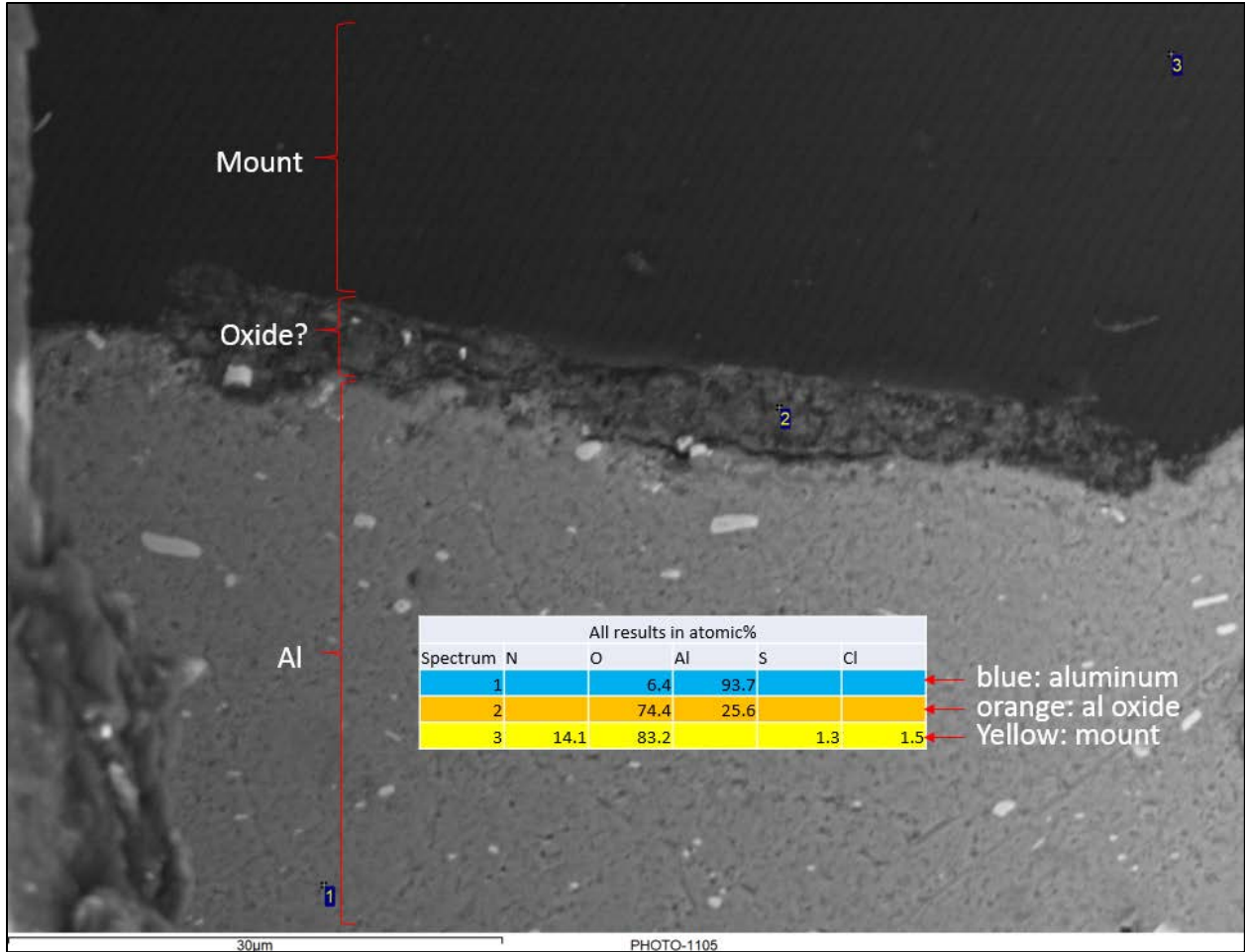
Figure 11 BSD image showing possible oxide layer at 1500X magnification.

3.4 FESEM on nickel-plated sample

Sample 1 (Figure 3) was mounted in EpoFix after the oxide surface was nickel-plated. In general, the cross-sectional oxide image appears well defined owing to the contrast created by the nickel-plating applied prior to mounting and polishing (Figure 12). Figure 13 provides a magnified view of the oxide and the nickel plating, revealing that some nickel migrated through cracks in the oxide during the plating process. The effect of this migration of nickel through the oxide on the oxide structure is unknown. Furthermore, the oxide layer in Figure 13 appears to have a layered structure. This layered structure may be indicative of episodic oxide growth. The overall oxide thickness in Figure 13 is 2 µm. EDS performed at point 2 in Figure 13 provides an O/Al ratio of ~2.8, which is consistent with $Al(OH)_3$ (gibbsite or bayerite).

Figure 12 Sample 1 BSD image showing "Ni droplet" on surface of oxide at 796X magnification.

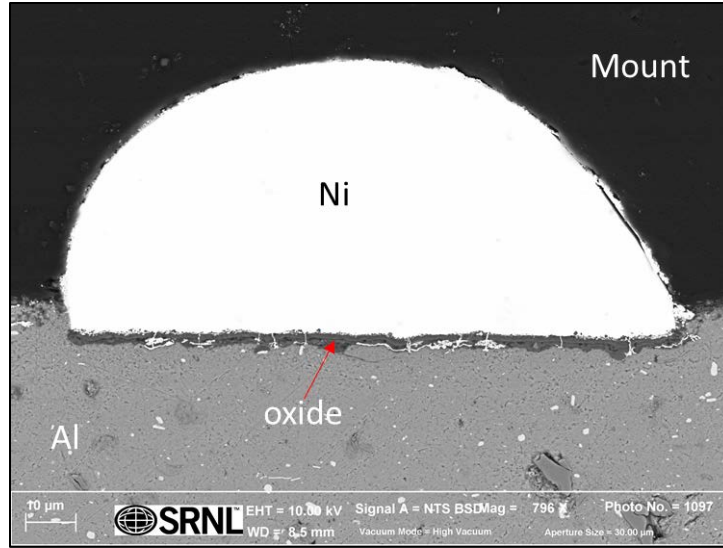|			All results in atomic%			
Spectrum	O	Al	Si	P	S	Ni
1	3.7			8.4		87.9
2	68.2	24.2	2.1	4.4	1.1	0.0
3	38.8	16.3	0.5	6.9	0.5	37.1
4	12.4	87.6				
5	6.2	93.8				

green: Ni plating (P is characteristic of electroless Ni)

orange: aluminum oxide

green: Ni plating and aluminum oxide

blue: aluminum, #5 is further away from oxide so less contribution to signal
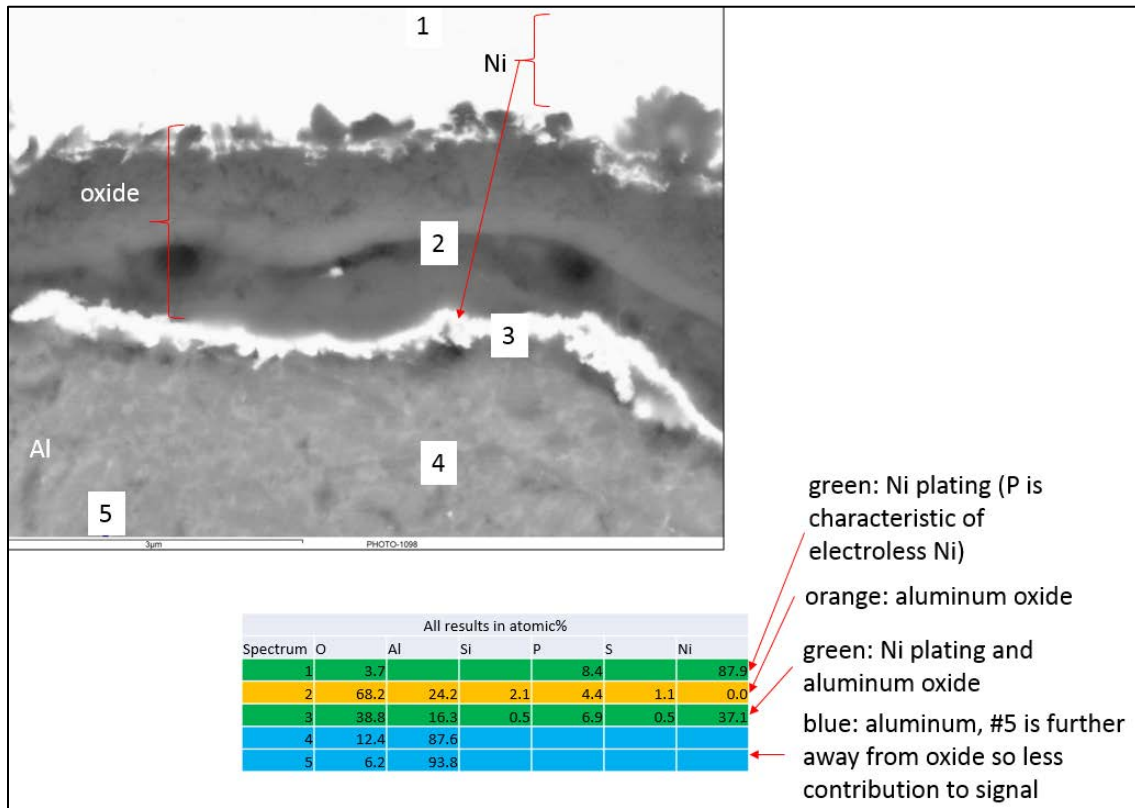
Figure 13 Sample 1 BSD image and EDS analysis of Al, oxide, and nickel surfaces (15,560X magnification)

An EDS line scan was performed through the oxide as shown in Figure 14, with the EDS line-scan overlaid on an SEM image in Figure 15. These figures show how the EDS spectra change as measured across a thick oxide. The high oxygen levels of the mounting material likely contribute to the oxygen signal for the first few points into the oxide near the mounting material. As observed in Figure 13, it is apparent that the nickel migrated through the oxide and reached the region between the oxide and the aluminum surface. The oxide thickness in Figure 14 ranged from 0.5 µm to 9.6 µm. In Figure 14, the O/Al ratios at EDS points 4

(O/Al=2.27), 5 (O/Al=1.99), 6 (O/Al=2.3), 7(O/Al=3.85), and 8 (O/Al=3.27) indicate varying composition though the oxide thickness. Near the oxide-mount interface, the ratio is close to 2, suggesting AlOOH (boehmite) as the composition; however, near the oxide-Al interface, the ratio is higher (3+) suggesting Al(OH)$_3$ (gibbsite or bayerite).
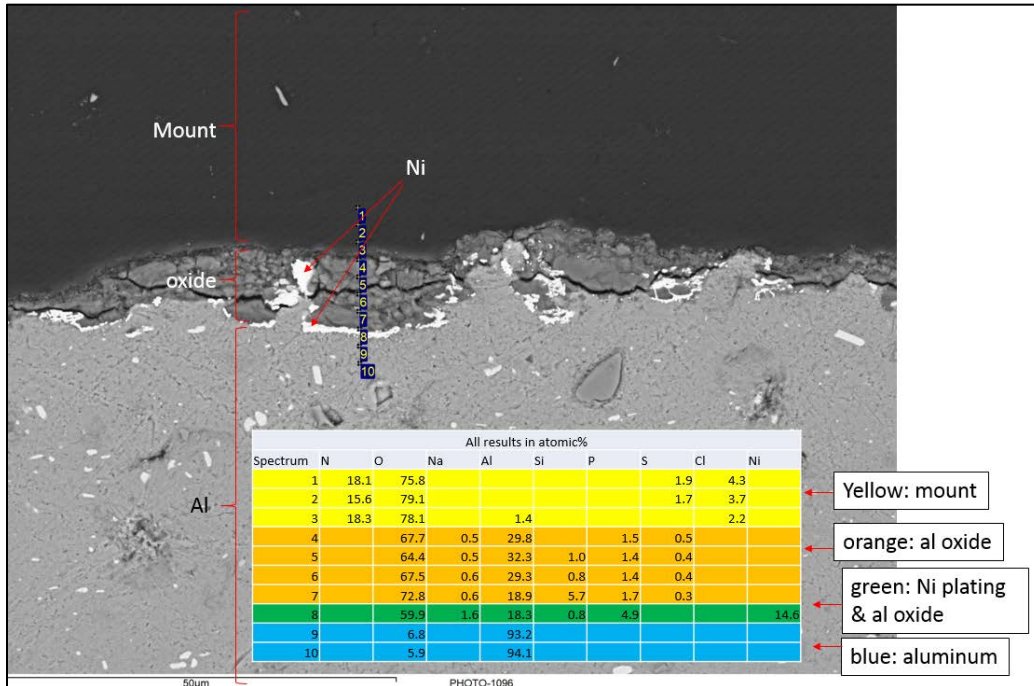
Figure 14 Sample 1 BSD image and EDS analysis of Al, oxide, and nickel surfaces (1000X magnification).
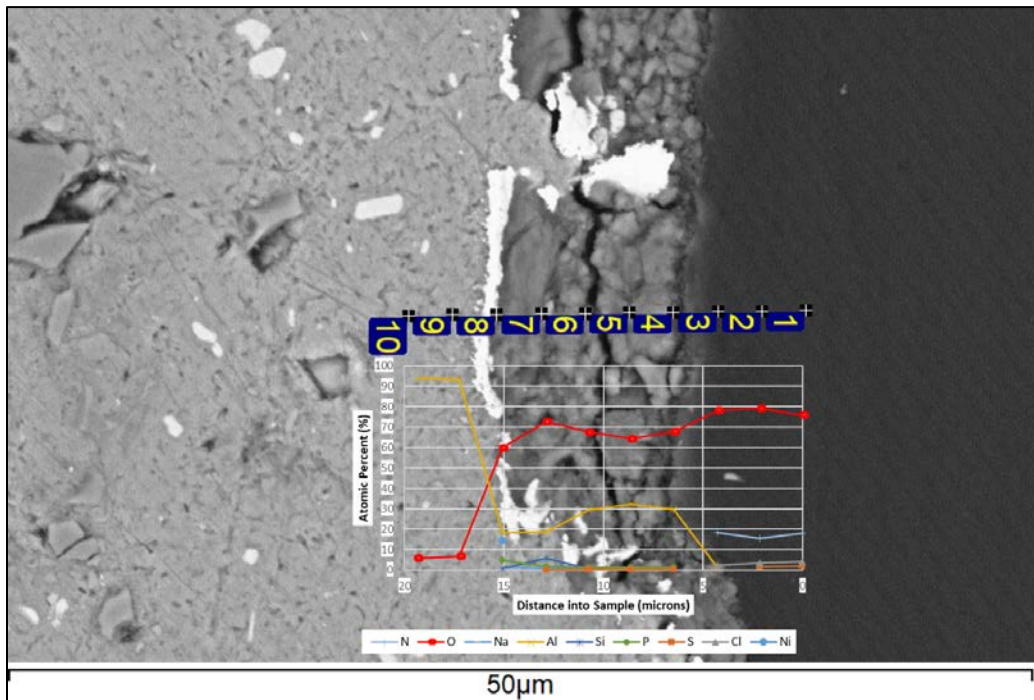
Figure 15 Sample 1 EDS line-scan overlaid on BSD SEM image of oxide.

In other regions, a thin oxide layer of ~ 200 nm in thickness was retained on the nickel-plated samples, Figure 16. The EDS point scan indicates that the thin film between the Al and the nickel-plate is an oxide, but the EDS signal also has a large contribution from the nickel-plating and the Al substrate.

Figure 16 BSD image and EDS analysis of Al, oxide, and nickel surfaces (13600X magnification).

3.5 <u>SEM Plan-View Thin Oxide</u>
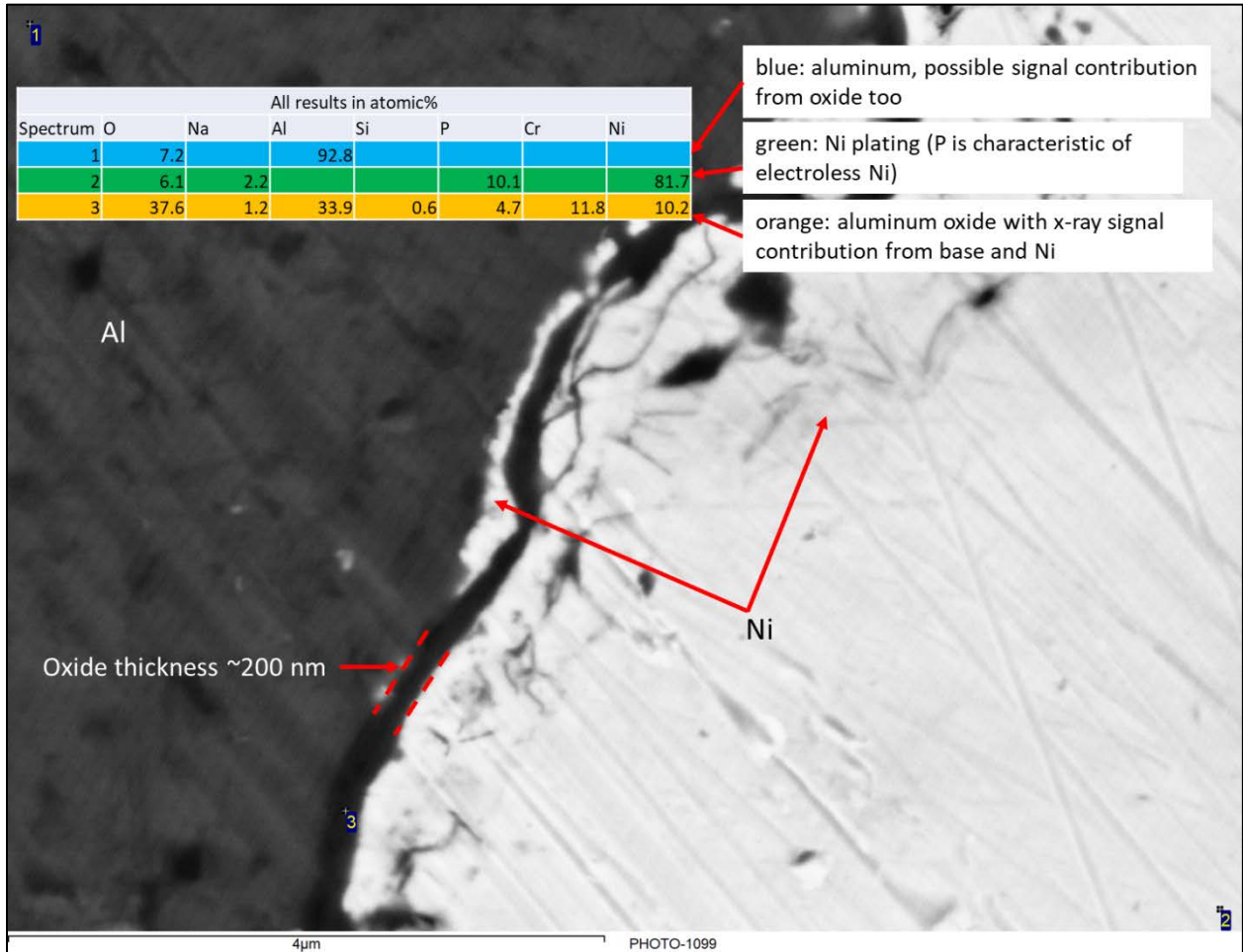
Most of the RU-1 sample surfaces were covered in a thin oxide layer, shown in cross-section in Figure 16, with thicker oxides sparsely present on the surface. From the SEM images observed previously, the majority of the RU-1 surface appeared to be covered in a thin oxide layer, ~200 nm thick, with occasional oxides ranging from ~5 to ~25 microns thick. Figure 17 shows a plan-view of this thin oxide. The thin oxide appears to be blocky and dense. The ~200 nm thick oxide is thinner than predicted from the model in section 2.3, which predicted an oxide thickness of 4-5 µm. However, Draley et al. [2] also reported that when oxides broke off, the underlying Al retained a shiny appearance and did not significantly regrow oxide, indicating that a thinner, more passive oxide would remain after sloughing. Also, as mentioned in section 2.3, Kim et al. [5, 6] reported thicker oxides (~10-45 µm) in practice on fuel exposed to similar temperature and pH conditions with the addition of water flow past the fuel.

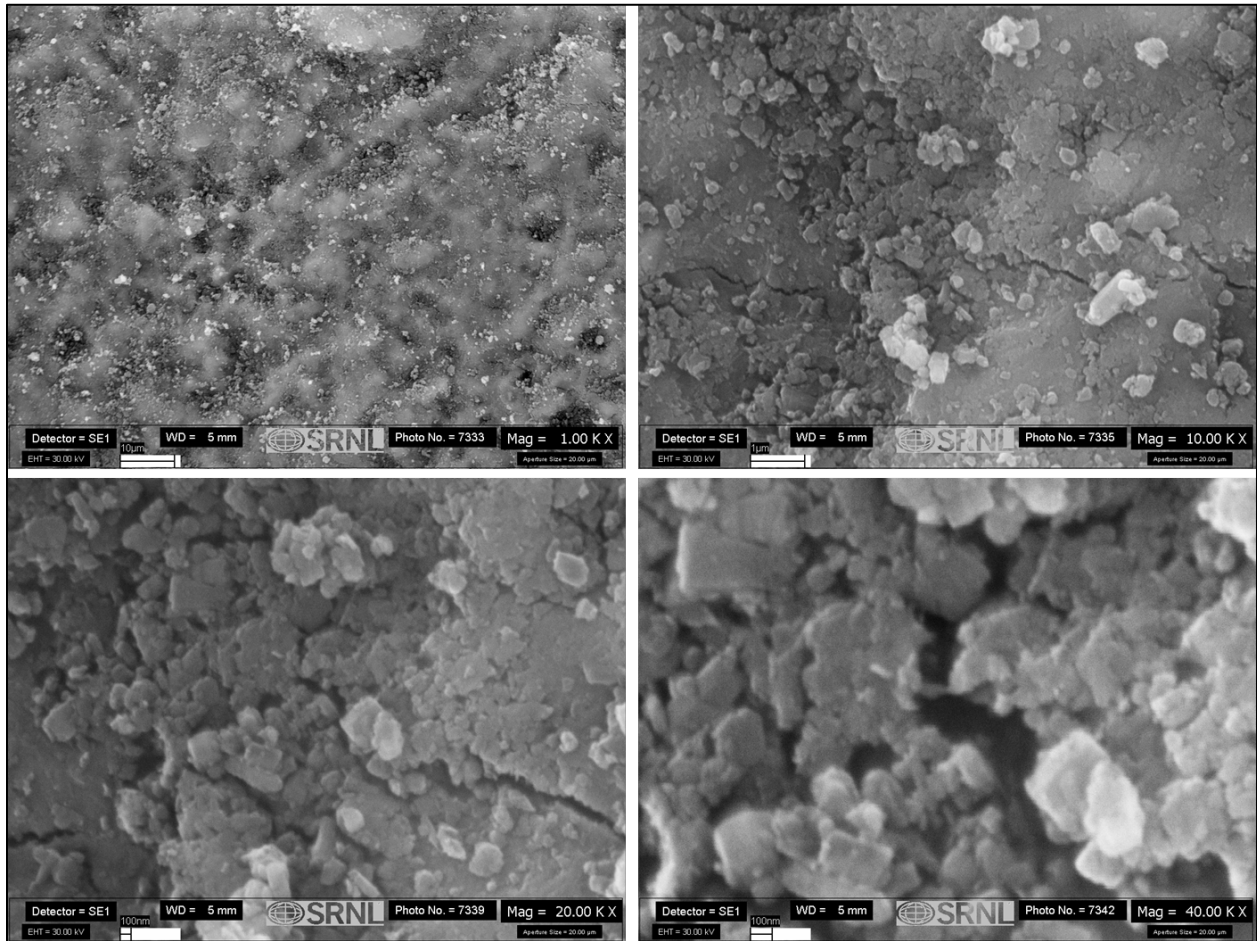**Figure 17 Thin oxide plan-view at several magnifications.**

3.6 SEM Plan-View Thick Oxide

Figure 18 shows a plan-view of a region of thicker oxide. Like the thin oxides, the thicker oxides also had a blocky and dense appearance. In fact, the morphology of the thick and thin oxides appears to be indistinguishable at high magnification.
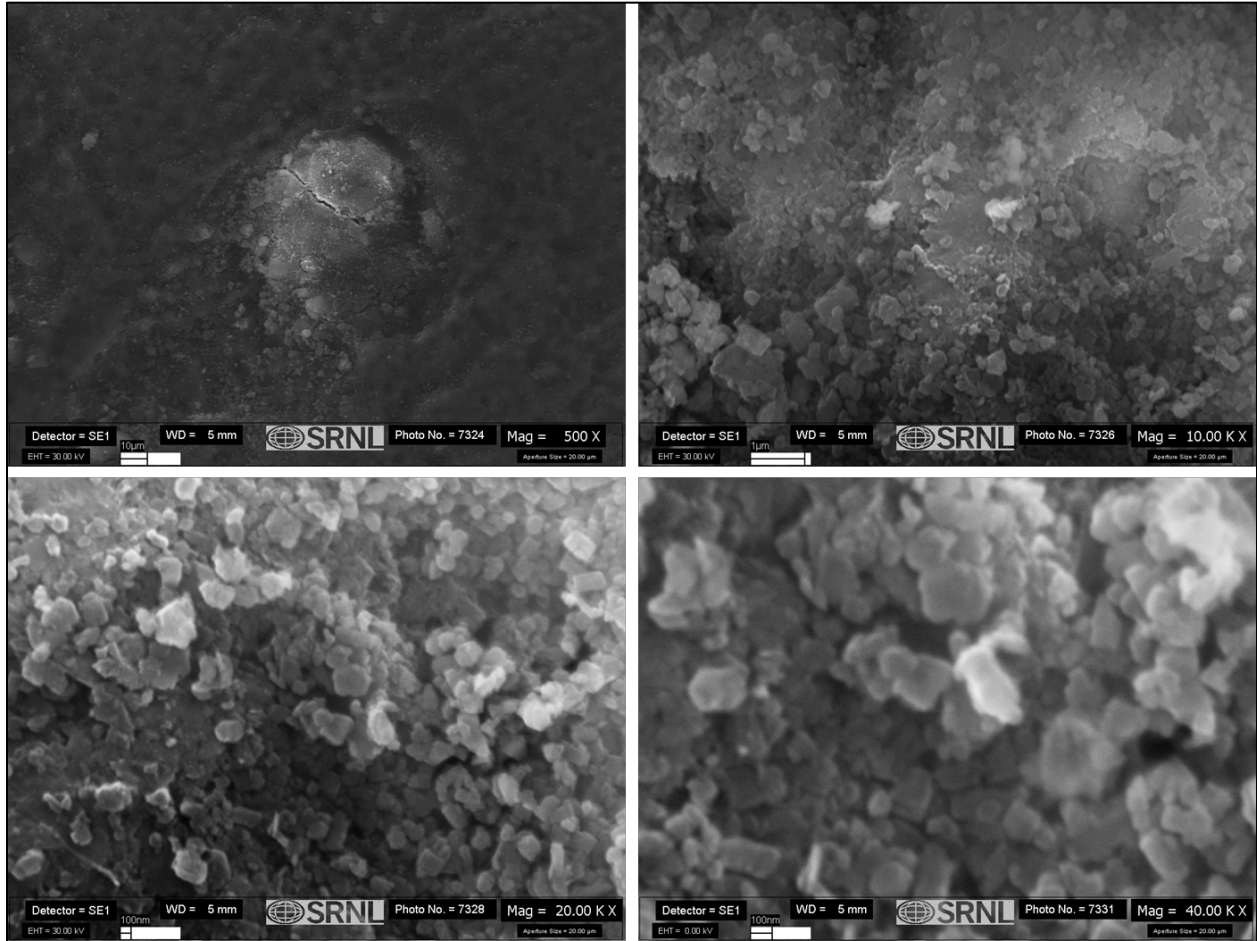

Figure 18 Thick oxide plan-view at several magnifications.

Figure 19 shows plan-view EDS point scans on the surface on the thin oxide as well as several of the thicker oxide patches. Due to topological and orientation effects of the electron beam, sample, detector, and unknown underlying substrates, the EDS results could have large error. In the EDS results in Figure 19, the oxygen and aluminum results are highlighted yellow for what are believed to be thick oxides, and other elements are highlighted orange which are above 1% atomic concentration but not aluminum or oxygen.

All results in atomic%

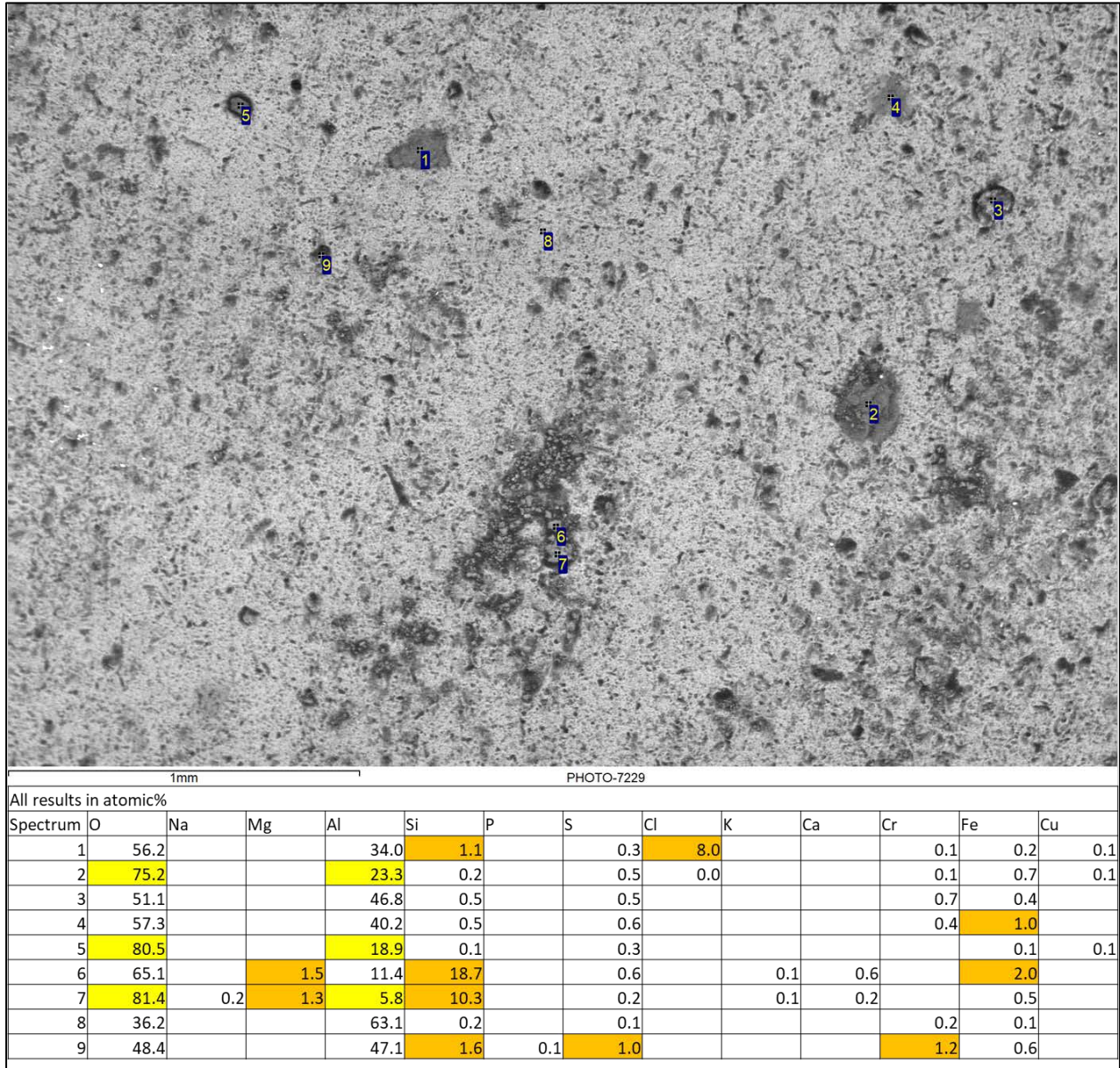| Spectrum	O	Na	Mg	Al	Si	P	S	Cl	K	Ca	Cr	Fe	Cu
1	56.2			34.0	1.1		0.3	8.0			0.1	0.2	0.1
2	75.2			23.3	0.2		0.5	0.0			0.1	0.7	0.1
3	51.1			46.8	0.5		0.5				0.7	0.4	
4	57.3			40.2	0.5		0.6				0.4	1.0	
5	80.5			18.9	0.1		0.3					0.1	0.1
6	65.1		1.5	11.4	18.7		0.6		0.1	0.6		2.0	
7	81.4	0.2	1.3	5.8	10.3		0.2		0.1	0.2		0.5	
8	36.2			63.1	0.2		0.1				0.2	0.1	
9	48.4			47.1	1.6	0.1	1.0				1.2	0.6	

Figure 19 SEM plan-view with EDS points and corresponding composition results.

4.0 Summary of Results

Oxyhydroxides were sampled from the cladding surface of dry-stored fuel plate from the RU-1 pool type reactor in Uruguay. FESEM with EDS, contained SEM with EDS, and XRD were performed on sectioned pieces of the fuel to evaluate the composition and thickness of oxides on the cladding surface. The observations from this work will in a future report be compared to characterizations of oxide films grown on alloys in the laboratory under prototypic conditions. Observations and results are provided below:

- The presence of oxides was identified with XRD and confirmed via EDS in both as-cut and nickel-plated mounted and polished sample cross-sections.
- The EpoFix mounting medium appeared to shrink and pull away from the sample upon curing. This led to a ravine in the non-plated sample and may have caused cracking in the oxide in the nickel-plated sample.
- XRD analysis revealed gibbsite as the predominant oxide on the fuel plate surface. It is possible that some boehmite may be present, as well, however the peak appears shifted.
- Most of the nickel-plated sample had only very thin oxide (~200 nm thick), as shown in Figure 16. The thin oxides were observed on the nickel-plated sample, but not in the as-cut and mounted/polished sample. This may be due to damage or contamination of the thin oxide during the epoxy-mounting process. In general, the oxides were more readily visible in the nickel-plated sample. However, the potential for the nickel plating process exposure to change the native oxide chemistry and morphology is unknown.
- Areas with thicker oxides up to 22.3 µm thick, e.g., Figure 12 through Figure 15, were observed sparsely on the surface of both the nickel-plated and unplated samples and may be considered outliers. The (thick) oxide in the nickel-plated sample in Figure 13 appears to have some layered structure. This layered structure may be indicative of episodic oxide growth.
- A logarithmic growth model from Draley et al. [2] predicted a (dense-oxide) thickness of 4-5 µm for an exposure duration of 5.75 years, the amount of time the fuel was under power in the reactor, while Kim et al. [5] reported oxide thicknesses of about 10-40 µm thick for reactors with forced water flow (8-9 m/s) at ~70 ± 20 °C, consistent with the thicknesses of the thick oxide regions.
- Draley et al. [2] also refer to previous findings of aqueous corrosion of 1100, stating that "After sufficiently extended exposure, bits of the corrosion product slough or flake off, leaving a metallic sheen. The corrosion product does not again grow thick in those places, and there is no observable increase in corrosion of the specimens." A similar process might be involved in thin oxide regions on the RU-1 if oxide remains thin after sloughing off.
- Plan-view observation of the fuel surface shows a blocky oxide morphology. The morphology appears to be the same for both the thin and thick oxide regions. Blocky films appear more dense and continued film growth in dense film would be expected to be slower due to contact with corrodent (water).

5.0 References

[1]   Herrera, "DOESRAAF-98-012 Rev. 7, Appendix A," *approved and issued under memo SFS-RSE-98-0093,* July 9 1998.

[2]   J. E. Draley, Mori, S., Loess, R. E. , "The Corrosion of 1100 Aluminum in Oxygen‐Saturated Water at 70° C," *Journal of The Electrochemical Society,* vol. 110, pp. 622-627, 1963.

[3]   K. Wefers and C. Misra, "Oxides and hydroxides of aluminum," Alcoa Laboratories Pittsburgh, PA Alcoa Technical Paper #19, 1987.

[4]   J. E. Draley, Mori, S., & Loess, R. E., "The Corrosion of 1100 Aluminum in Water from 50° to 95°C," *Journal of The Electrochemical Society,* vol. 114, pp. 353-354, 1967.

[5]   Y. S. Kim, Hofman, G. L., Hanan, N. A., Snelgrove, J. L. , "Prediction model for oxide thickness on aluminum alloy cladding during irradiation," in *2003 International Meeting on Reduced Enrichment for Research and Test Reactors*, 2003.

[6]   Y. S. Kim, Hofman, G. L., Robinson, A. B., Snelgrove, J. L., Hanan, N., "Oxidation of aluminum alloy cladding for research and test reactor fuel," *Journal of Nuclear Materials,* vol. 378, pp. 220-228, 2008.

[7]   Caswell. (September 26). *Electroless Nickel Mini Kit (5 Pint).* Available: https://www.caswellplating.com/electroplating-anodizing/nickel-plating-kits/electroless-nickel-mini-kit-5-pint.html

[8]   B. Rabin, M. Meyer, J. Cole, I. Glagolenko, G. Hofman, W. Jones*, et al.*, "Preliminary Report on U-Mo Monolithic Fuel for Research Reactors," Idaho National Laboratory INL/EXT-17-40975, 2017.

[9]   K. E. Metzger, R. Fuentes, A. d'Entremont, L. Olson, and R. Sindelar, "Preparation of aluminum oxide films under water exposure - Preliminary report on 1100 series alloys," Savannah River National Laboratory SRNL-STI-2018-00427, 2018.

[10]   A. L. d'Entremont, R. E. Fuentes, L. C. Olson, and R. L. Sindelar, "Preparation of Aluminum Oxide Films Under Water Exposure – Preliminary Report on 6061 Series Alloys," Savannah River National Laboratory SRNL-STI-2018-00449, 2018.

[11]   M. Dewar, "Characterization and Evaluation of Aged 20Cr32Ni1Nb Stainless Steels," Master of Science in Materials Engineering, Department of Chemical and Materials Engineering, University of Alberta, Edmonton, Alberta, 2013.

[12]   J. Goldstein, Newbury, D.E., Joy, D.C., Lyman, C.E., Echlin, P., Lifshin, E., Sawyer, L., Michael, J.R., *Scanning Electron Microscopy and X-Ray Microanalysis*.

Distribution:

SRNL:

Records Administration (EDWS)

william.bates@srnl.doe.gov

Matthew.Garrett@srnl.doe.gov

kristine.zeigler@srnl.doe.gov

Marissa.Reigel@srnl.doe.gov

Brenda.Garcia-Diaz@srnl.doe.gov

bruce.wiersma@srnl.doe.gov

anna.dentremont@srnl.doe.gov

Roderick.Fuentes@srnl.doe.gov

Luke.Olson@srnl.doe.gov

robert.sindelar@srnl.doe.gov

ps.lam@srnl.doe.gov

INL:

michael.connolly@inl.gov

josh.jarrell@inl.gov